

Singing in the Wind: Numerically Solving the Navier-Stokes Equations with Movable Boundary Conditions

Dylan Hamilton

The College of Wooster, Wooster, Ohio 44691, USA

(Dated: May 12, 2016)

A simulation was created to solve the Navier-Stokes equations for a moving object accelerated by a fluid. The program expanded upon a previously written program that solved the Navier-Stokes equation for stationary boundary conditions using an imported inverse Lagrangian matrix. The new program inverts the Lagrangian numerically, using a freely available c++ library that enables fast and efficient large sparse square matrix inversion. The acceleration of the object by the the fluid is calculated by summing up the pressures around the object and calculating the acceleration due to this net pressure. The Lagrangian is then recalculated every time the object moves. The physical validity of the simulation was confirmed by constraining a circular object to movement in the y-direction pulled by a spring, which modeled a 2-D cross section of a telephone wire in the wind. The simulation reproduced the experimental results of the wire being forced into sinusoidal-like motion transverse to the wind velocity.

I. INTRODUCTION

The study of fluids is both complex and highly important. Unlike solids, which maintain their shape and move somewhat predictably when pushed or pulled, fluids change their shape and even their density in complex ways. Additionally, if a solid is moving in a given direction, then each of it's parts is moving with the same velocity. A fluid, on the other hand, may be moving as a whole in a given direction with parts of it moving in opposite directions or transverse directions [1]. Because of their complexity, fluids lead to some very interesting and important phenomena when coming into contact with solids, including *lift* and *vortex shedding*. Vortex shedding is a phenomenon in which, for fluids with Reynolds numbers between 40 and 300 [2], the development of symmetric vortices directly behind the object is followed by vortices periodically swirling off of either side of a cylinder in a fluid flow, as seen in Fig. 1. These phenomena are vital to explaining many important things, including windmills, airplanes, race cars, weather, and the eerie tone sometimes generated by telephone wires "singing in the wind" [1–4].

This work continues the work done by Danielle Shepherd in which a computer program which numerically solved the Navier-Stokes equations for fixed boundary conditions was written from the ground up [4]. With the



FIG. 1: Vortices alternately shedding off of a circular object in a fluid flow. This figure is reproduced from reference [3].

completion of her program, it was verified that the simulation did indeed reproduce experimental results by the observation of vortex shedding around a fixed approximate circle in a fluid flow. However, in her program this object was fixed in place, unable to respond to the forces produced by the interaction between the object and the fluid. This restriction therefore severely limited the application of the program, as it could not model a system in which the object could move if blown by the wind. The obvious next step in the development of the program, then, was to allow for the object to move in response to the forces on it by the fluid. To confirm that the program was correctly simulating physical phenomena, a known scenario, that of a telephone wire oscillating transversely to the wind, was simulated for. The motion of the simulated telephone wire was then compared to the motion of a physical one, and it was verified that the motions matched each other.

This report will first discuss the incompressible Navier-Stokes equations in conservation form. Then it will address the importance of the inverse Laplacian in solving for the pressures of the system simultaneously. Also discussed will be the calculation of the acceleration of the object due to a pressure gradient. Subsequently, the methodology of the simulation will be discussed, first addressing the need for large sparse matrix inversion and then addressing the method in which the object was moved and tracked. Finally, the results will be discussed in which the simulation was validated by correctly simulating a 2-D cross section of a telephone wire oscillating transversely to the wind.

II. THEORY

A. Navier-Stokes Equations

The Navier-Stokes equations are a pair of coupled equations of motion for an isotropic Newtonian fluid [4]. They rely on three physical principles: (1) Newton's sec-

ond law, (2) conservation of energy, and (3) conservation of mass [1]. In addition, they assume a continuum model of a fluid in which the fluid is infinitely divisible into small parts with equal properties [5]. The incompressible Navier-Stokes equations in conservation form are [1, 4, 7]

$$\frac{\partial \vec{v}}{\partial t} = -(\vec{v} \bullet \vec{\nabla})\vec{v} - \frac{1}{\rho} \vec{\nabla} P + \nu \nabla^2 \vec{v} \quad (1a)$$

$$0 = \vec{\nabla} \bullet \vec{v}, \quad (1b)$$

where \vec{v} is the velocity of the fluid, ρ is the density, P is the pressure, and ν is the kinematic viscosity. The first equation relates the local change in velocity with time to three terms. The second term relates it to the pressure gradient, an alternate form of Newton's second law. The first term then subtracts out the non-local change in velocity, or the change in velocity of the fluid based solely on the movement of the fluid element from one location to another. Finally the third term is a frictional term, accounting for an acceleration opposite the divergence of the velocity, based on the kinematic viscosity ν , the fluid equivalent of the coefficient of friction. The second equation is considerably simpler: because the fluid is incompressible, the change in density of the fluid must be zero, and thus the divergence of the velocity of the fluid must also be zero.

B. The Laplacian

In observing the Navier-Stokes equations, it is clear that there are two unknowns that we are solving for: the change in velocity with time and the pressure gradient. To solve for the updated velocity at time $t + dt$, we take

$$\vec{v}(t + dt) = \vec{v}(t) + \frac{\partial \vec{v}}{\partial t} dt. \quad (2)$$

The local acceleration ($\partial \vec{v} / \partial t$) of the fluid is solved for in the first of the Navier-Stokes equations (Eq. 1a). Thus, substituting this in to Eq. 2 yields

$$\begin{aligned} \vec{v}(t + dt) &= \vec{v}(t) - (\vec{v} \bullet \vec{\nabla})\vec{v} dt - \frac{1}{\rho} \vec{\nabla} P dt + \nu \nabla^2 \vec{v} dt \\ \vec{v}(t + dt) &= \vec{v}_i - \frac{1}{\rho} \vec{\nabla} P dt \end{aligned} \quad (3)$$

where $\vec{v}_i \equiv \vec{v}(t) - (\vec{v} \bullet \vec{\nabla})\vec{v} dt + \nu \nabla^2 \vec{v} dt$ can be thought of as an intermediate velocity term. In computing the updated pressure values, the second of the Navier-Stokes equations (Eq. 1b), namely that the velocity field must not diverge, must be satisfied simultaneously. Thus, by

applying this principle and solving for P , it follows

$$\begin{aligned} 0 &= \vec{\nabla} \bullet \vec{v}(t + dt) \\ &= \vec{\nabla} \bullet \left(\vec{v}_i - \frac{1}{\rho} \vec{\nabla} P dt \right) \\ &= \vec{\nabla} \bullet \vec{v}_i - \vec{\nabla} \bullet \left(\frac{1}{\rho} \vec{\nabla} P dt \right) \\ &= \vec{\nabla} \bullet \vec{v}_i - \frac{1}{\rho} \nabla^2 P dt \\ \nabla^2 P &= \left(\vec{\nabla} \bullet \vec{v}_i \right) \frac{\rho}{dt} \\ P &= \nabla^{-2} \left(\vec{\nabla} \bullet \vec{v}_i \right) \frac{\rho}{dt}. \end{aligned} \quad (4)$$

Thus, in order to solve for the pressure, the inverse Laplacian must be calculated. This is discussed further in the methodology section.

C. Acceleration of the Object Due to a Pressure Gradient

The acceleration of the object due to a net pressure difference on its sides needs to be calculated in order to be able to calculate the motion of the object. From Newton's second law $\vec{F} = m\vec{a}$ and the definition of pressure $P = \vec{F}/\vec{A}$, it can be shown that

$$\begin{aligned} m\vec{a} &= P\vec{A} \\ \vec{a} &= \frac{P\vec{A}}{m} \\ \sum \vec{a} &= \frac{1}{m} \sum (P\vec{A}). \end{aligned} \quad (6)$$

Thus, by simply summing up the pressures around the object, the acceleration of the object due to a pressure gradient can be obtained.

III. METHODOLOGY

In solving the Navier-Stokes equations, the Laplacian, a very large sparse square matrix that describes the boundary conditions, must be inverted to then solve simultaneously for the pressures at all cells using Eq. 5. Shepherd's program implemented a novel technique: she solved exactly for the inverted Laplacian using Mathematica, and then imported the inverted Laplacian into her program [4]. This was unique to the field, because other programs numerically invert the Laplacian using a method such as LU Decomposition rather than exactly invert it in Mathematica.

Because the Laplacian describes the boundary conditions, for fixed boundary conditions it stays constant throughout the simulation and only needs to be inverted once. For movable boundary conditions, however, it must be recalculated every time the boundary conditions change. Thus, the new program needed to be able

to solve a large sparse square matrix automatically and quickly. While it would have been possible to continue with Shepherd’s use of Mathematica to invert the Laplacian if correctly automated, due to the overhead in starting and running a separate program every time the Laplacian needed to be inverted, it was decided to implement an available c++ matrix solver especially optimized to rapidly solve particularly sparse matrices. The chosen solver was Eigen, a free c++ template library for linear algebra [6]. The code was then modified to use the syntax and structures native to Eigen.

A method was then written to calculate the movement of the object. This method is rather simple. First, it scans through every fluid cell that is not on the outside border. If the fluid cell is adjacent to an object cell, the pressure of the fluid cell is added (with the correct direction) to the pressure vector that is the sum of all pressures on the object. Using Eq. 6 to calculate the acceleration of the object due to the pressure, an Euler-Cromer algorithm is then implemented to calculate the displacement.

There are two location grids in the simulation: the fluid grid and the simulation grid. The fluid grid is the grid of fluid cells, where the Navier-Stokes equations are used to calculate the pressure and velocity of the fluid in each cell. This grid is actually a staggered grid made up of a primary and secondary grid that are offset from each other, with the pressure calculated on the primary grid and the velocity calculated on the secondary grid. (See references [4] and [7] for more information on the importance and on the implementation of a staggered grid.) The simulation grid, on the other hand, can be thought of as one with spacings down to double precision which keeps track of the position, velocity, and acceleration of the object. Because the fluid grid is so much more coarse than the simulation grid, the position of the object can change notably in the simulation grid without having moved enough to change in the position grid. Thus, the position, velocity and acceleration of the object are all summed up over multiple iterations in the simulation grid. Then, only once the object has moved by more than half of a cell in the cell space does the cell grid get updated, the Laplacian recomputed, and the Navier-Stokes equations applied to the new boundary conditions.

IV. RESULTS

A preliminary set of images from the completed simulation is displayed in Fig. 2. In the figure, the circular object (black) is constrained to motion by a spring in the y-direction, simulating a 2-D cross section of a telephone wire in the wind which has been shown to move in an oscillatory motion transverse to the wind [2, 3]. To simplify and speed up the simulation, it was assumed that in the x-direction, a steady state had already been reached where the force in the x-direction on the wire by the wind was equal to the force in the opposite direction from the

tension in the wire. The motion that was allowed for then was the motion transverse to the wind. This motion has been explained theoretically by an oscillatory force due to vortices shedding alternately off either side of the disk [2, 3].

The motion in Fig. 2 is indeed that described by alternate vortex shedding. The velocity vectors are color coded according to the legend in Fig. 3. Frame (a) of Fig. 2 is just as the fluid starts to flow around the object. In frame (b), early, symmetric vortices are formed. Frame (c) shows the vortices shedding off the bottom of the cylinder take over, and the object is forced downward. In frame (d), the object has slowed and the development of a vortex shedding off of the top of the object is seen in the blue/purple at top/right of the object. These top-shedding vortices are further developed in frames (e) and (f) and push the object upward. Frame (g) shows a little “blip,” where the object is slowed by a vortex developing on the bottom of the object. This vortex is short lived, and the object continues in an upward motion being forced by the vortices shedding off of the top of the object in frames (h) and (i). In frame (j), the object reaches the top of its displacement and turns around, as the development of a bottom-shedding vortex is seen in yellow at the bottom right of the object. This bottom-shedding vortex takes over in (k) and forces the object downwards in (l) and (m). In frame (n), the object reaches the bottom of its displacement as top-shedding vortices develop in blue at the top right of the object. These top-shedding vortices take over and start forcing the object upward again in frame (o).

It is interesting to note that, in Fig. 2, while the object is in motion in a particular direction, the motion seems to encourage the type of vortex shedding that increases that direction of motion. For example, as the object moves upward, the vortex forming that is encouraged is the top-shedding which continues to force the object upward until it is pulled to a top by the spring. While moving, then, the vortex shedding doesn’t seem to alternate as it does while the object is stationary as in Fig. 4.

These alternating shedding vortices can be seen without the movement of the disk in Fig. 4. In this simulation the spring was stiff enough (with $k = 3 \times 10^8$ in arbitrary units) for the object not to move more than half a fluid cell (and thus change the boundary conditions), yet the pressures and movement of the center of the disk on the simulation grid were recorded. Fig. 5 shows the position of the disk (red) with a fitted sinusoidal wave (blue). It can be seen that the displacement and thus the forcing by the shedding vortices for a stationary object (as far as the fluid was concerned, the object was stationary because it didn’t move on the fluid grid because it wasn’t displaced by more than half of a cell length) is quite sinusoidal.

Fig. 6 shows the displacement (red) in the y-direction of the center of the object over time for the disk attached to a spring with $k = 2 \times 10^8$ in arbitrary units. The beginning and the “blip” described in Fig. 2 are readily visible, however later the motion is largely sinusoidal. The blue

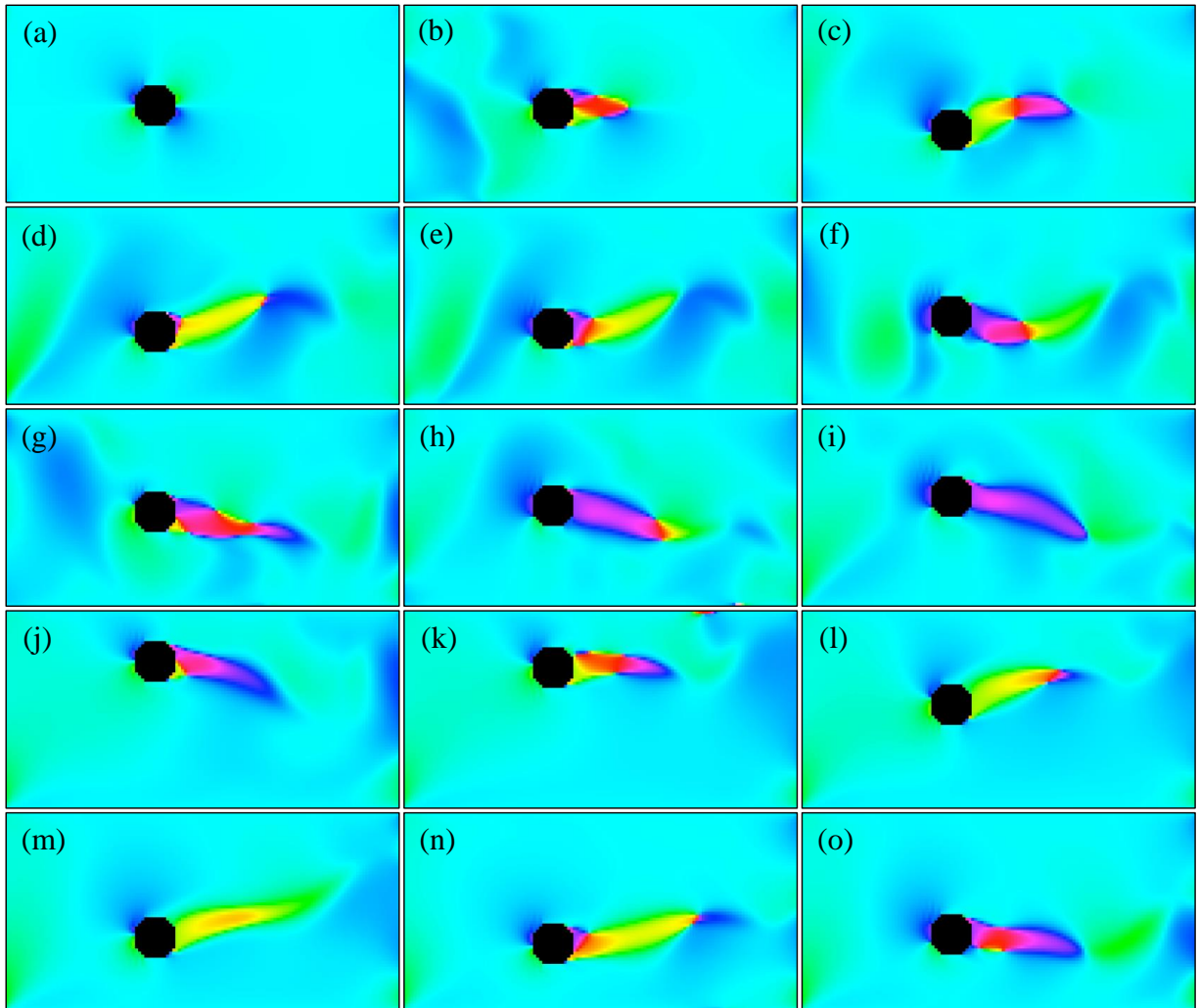


FIG. 2: The fluid flow around and motion of a circular object (black) constrained to motion in the y -direction by a spring of $k = 2 \times 10^8$ a.u. After the development of symmetric vortices in frame (b), the vortices alternately shed off the top and the bottom of the object, forcing it to oscillate up and down.



FIG. 3: The color coded velocity legend. The colors describe the direction of the velocity of the fluid while the saturation describes the magnitude. For example, the aqua blue color is fluid moving to the right and the red is fluid moving backwards, with the darker red fluid moving at a greater velocity than the paler red.

curve shows a sinusoidal curve fit to the displacement from about $t = 733$ a.u., the point at which the displace-

ment appears to start being sinusoidal. These results make physical sense: at the parameters in which a telephone wire starts “singing” a mostly pure tone, we would expect the motion of the wire to be sinusoidal, similar to a vibrating violin string. Thus, the sinusoidal behavior of the shedding vortex-forced disk suggests that we are in the parameter regime of singing wires, that the wire is indeed singing, and thus that our simulation is qualitatively reproducing known physical effects of a wire in an airflow!

V. CONCLUSION

The sinusoidal motion in time of the disk confirm that it is correctly simulating physical phenomena. However, there is still much to be done before the simulation can be used to gain real insight into physical scenarios. First, the relationship between simulation units and real units

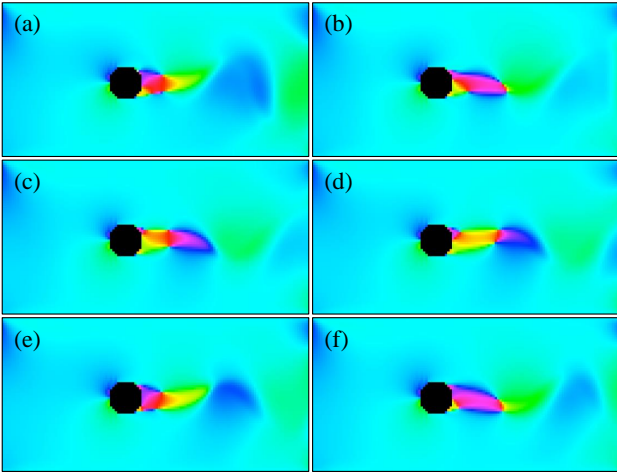


FIG. 4: The fluid flow around a circular object constrained to motion in the y -direction by a spring of $k = 3 \times 10^8$. During the time period shown with the given spring stiffness, the vortices alternate too rapidly to do enough work on the object to move it by more than one fluid cell. Thus, on the fluid grid, the object is stationary. Frames (a) through (f) show the alternating vortices shedding off the top and bottom of the object.

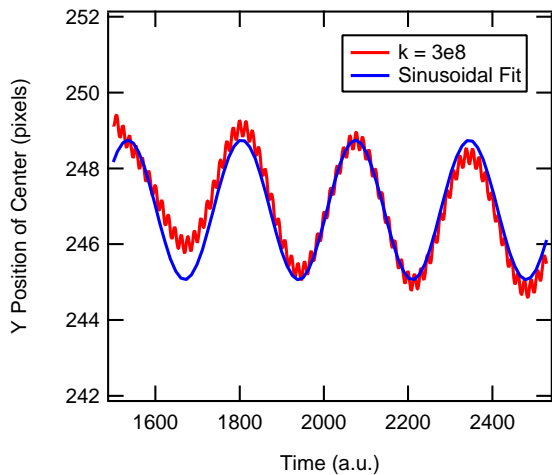


FIG. 5: Y Position vs Time for a Stationary Object. In this plot, “stationary” is in the view of the fluid grid, in which the object never moves because it is never displaced by more than half of the width of one cell. Yet the position of the center on the simulation grid (shown) is always calculated. Because the position is sinusoidal with time, as it compares very well to the sine curve fit to the function (blue), it implies that the acceleration too is sinusoidal in time, and thus the sum of the forces by the alternately shedding vortices is periodic in time.

needs to be established. Second, while the simulation does simulate the effect of the fluid on the motion of the object, the simulation currently ignores the effect of the motion of the object on the fluid. Moving an object through a fluid certainly creates disturbance, such as a cone of separating water in front of the disk or the wake

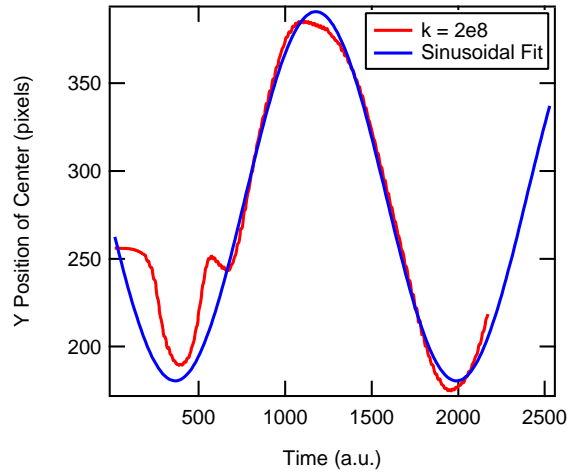


FIG. 6: Y Position vs Time for a Movable Object. After the first blip, the displacement aligns closely to the calculated sinusoidal fit curve (blue). This suggests harmonic motion and a basis for the “singing” telephone wires.

behind the moving object, yet this is not yet accounted for in the simulation. Given that, in this scenario, the velocity of the object is very slow relative to the velocity of the wind around it, this effect is probably relatively negligible. However, in a scenario where the object is moving faster relative to the velocity of the wind, these effects will need to be taken into account. Third, the current method of calculating the force on the object is to calculate the pressures of the fluid cells around it. However, the pressure values are the pressures for the center of the fluid cell, not the border of the cell touching the object. Indeed, it was for the very reason that these bordering pressures are not known that a staggered grid was used [4, 7]. Thus, it is uncertain for what regime this method of calculating the net force on the object will remain accurate.

An eventual goal of this project might be the simulation of vertical axis wind turbines. However, if this is to be accomplished, the interaction between the wind and the turbine blade must be very accurate in order to be able to predict the efficiency of certain blade designs in comparison to others. Yet the current resolution is very far from affording this accuracy, especially since the current simulation uses a square grid, and blades that create lift are far from square. In the future, it would be worth looking into different types of grids, such as a non-rectangular boundary fitted Eulerian (fixed) grid [1] or possibly an arbitrary Lagrangian-Eulerian grid: a boundary fitted grid that moves with the boundary in question [8, 9].

VI. ACKNOWLEDGMENTS

The author wishes to thank Dr. John Lindner and Dr. Susan Lehman for all of their guidance and expertise

throughout the project. He also wishes to thank Danielle Shepherd for allowing him to expand upon her work, for her great introduction to the Navier-Stokes equations, and for her ample code comments. He wishes to extend special thanks to Jackie Middleton for all of her work that

makes the physics program run smoothly. Finally, he wishes to thank all of the staff at the College of Wooster who work tirelessly in order to allow him to pursue his education.

-
- [1] J.F. Wendt *et al*, *Computational Fluid Dynamics: An Introduction*, 3rd Ed. (Springer-Verlag, Berlin, Germany, 2009), pp. 15-51.
- [2] R.D. Belvins, *J. Sound Vib.* **92**(4), 455 (1984).
- [3] S.C. Frautschi, R.P. Olenick, T.M. Apostol, and D.L. Goodstein, *The Mechanical Universe: Mechanics and Heat, Advanced Edition*, (Cambridge University Press, New York, NY, 2008), pp. 326.
- [4] D. Shepherd, *Go With the Flow: Developing Computational Fluid Dynamics Simulations According to the Navier-Stokes Equations*, (OpenWorks, The College of Wooster, Wooster, OH, 2014).
- [5] G.K. Batchelor, *An Introduction to Fluid Dynamics*, (Cambridge University Press, New York, NY, 2000), pp. 4.
- [6] G. Guennebaud, B. Jacob, and others, C++ Library Eigen v3, (<http://eigen.tuxfamily.org>, 2010).
- [7] D. Cline, D. Cardon, and P.K. Egbert, *Fluid Flow for the Rest of Us: Tutorial of the Marker and Cell Method in Computer Graphics*, (Technical Report, Brigham Young University, 2013).
- [8] F. Alouges and B. Maury, *Variational Methods for Computational Fluid Dynamics* (n.d.).
- [9] C.W. Hirt, A.A. Amsden, and J.L. Cook, *An Arbitrary Lagrangian-Eulerian Computing Method for All Flow Speeds*, *J. Comput. Phys.* **14**, 227 (1974).